

# Cardiotoxicity and Cardioprotection by Artesunate in Larval Zebrafish

Chuanrui Zheng<sup>1</sup> , Letian Shan<sup>1</sup> , Peijian Tong<sup>1</sup>, and Thomas Efferth<sup>2</sup>

Dose-Response:  
An International Journal  
January-March 2020: 1-13  
© The Author(s) 2020  
Article reuse guidelines:  
sagepub.com/journals-permissions  
DOI: 10.1177/1559325819897180  
journals.sagepub.com/home/dos



## Abstract

Although artesunate (ART) is generally accepted as a safe and well-tolerated first-line treatment of severe malaria, cases of severe side effects and toxicity of this compound are also documented. This study applied larval zebrafishes to determine the acute toxicity and efficacy of ART and performed RNA-sequencing analyses to unravel the underlying signaling pathways contributing to ART's activities. Results from acute toxicity assay showed that a single-dose intravenous injection of ART from 3.6 ng/fish (1/9 maximum nonlethal concentration) to 41.8 ng/fish (lethal dose 10%) obviously induced pericardial edema, circulation defects, yolk sac absorption delay, renal edema, and swim bladder loss, indicating acute cardiotoxicity, nephrotoxicity, and developmental toxicity of ART. Efficacy assay showed that ART at 1/2 lowest observed adverse effect level (LOAEL) exerted cardioprotective effects on zebrafishes with verapamil-induced heart failure. Artesunate significantly restored cardiac malformation, venous stasis, cardiac output decrease, and blood flow dynamics reduction. No adverse events were observed with this treatment, indicating that ART at doses below LOAEL was effective and safe. These results indicate that ART at low doses was cardioprotective, but revealed cardiotoxicity at high doses. RNA-sequencing analysis showed that gene expression of *frizzled class receptor 7a (fzd7a)* was significantly upregulated in zebrafishes with verapamil-induced heart failure and significantly downregulated if ART at 1/2 LOAEL was coadministrated, indicating that *fzd7a*-modulated Wnt signaling may mediate the cardioprotective effect of ART. For the first time, this study revealed the biphasic property of ART, providing in-depth knowledge on the pharmacological efficacy-safety profile for its therapeutic and safe applications in clinic.

## Keywords

cancer, malaria, natural products, network pharmacology, toxicology

## Introduction

As complementary and alternative medicine, traditional Chinese medicine (TCM) gains increasing popularity and attracts growing attention around the world. *Artemisia annua* L. (Asteraceae), known as *Qing Hao* in Chinese, is a famous TCM herb for clearing summer-heat, curing fever, and treating malaria.<sup>1</sup> It was firstly recorded in the earliest poetry anthology “*Classic of Poetry*” (*Shi Jing*) during the Spring and Autumn Period of China (770-476 BC). The medicinal property of this herb was originally described by the existing earliest pharmacopoeia “*Shennong Ben Cao Jing*” (*Shennong's Herbal*) during the East Han Dynasty of China (25-220 AD). *Artemisia annua* became very famous worldwide owing to the contribution of its bioactive component, artemisinin, for malaria control. A main investigator on the antimalarial artemisinin was Youyou Tu, who was conferred several prestigious awards, including the Lasker DeBakey Clinical Research Award (2011) and the Nobel Prize

for Medicine or Physiology (2015).<sup>2-4</sup> A semisynthetic derivative of artemisinin, artesunate (ART), was developed as first-line treatment of severe malaria in endemic countries by the World Health Organization.<sup>5</sup> In addition, numerous studies also pointed out that ART had widespread pharmacological activities, such as anticancer, anti-inflammatory, antiparasite,

<sup>1</sup> The First Affiliated Hospital, Zhejiang Chinese Medical University, Hangzhou, Zhejiang, People's Republic of China

<sup>2</sup> Department of Pharmaceutical Biology, Institute of Pharmacy and Biochemistry, Johannes Gutenberg University, Mainz, Germany

Received 24 September 2019; received revised 13 November 2019; accepted 26 November 2019

## Corresponding Author:

Thomas Efferth, Department of Pharmaceutical Biology, Institute of Pharmacy and Biochemistry, Johannes Gutenberg University, D-55128 Mainz, Germany. Email: efferth@uni-mainz.de



Creative Commons Non Commercial CC BY-NC: This article is distributed under the terms of the Creative Commons Attribution-NonCommercial 4.0 License (<https://creativecommons.org/licenses/by-nc/4.0/>) which permits non-commercial use, reproduction and distribution of the work without further permission provided the original work is attributed as specified on the SAGE and Open Access pages (<https://us.sagepub.com/en-us/nam/open-access-at-sage>).

antimicrobial, antioxidant, antiatherosclerotic, and immunoregulatory effects.<sup>6-14</sup> It has been found to exert anticancer effect by inducing cell apoptosis, antagonizing angiogenesis, reversing immuno-suppression of tumor cells.<sup>15</sup> In clinic, the anticancer effect of ART was prominent in subjects with many cancers. A single center, randomised, double-blind, placebo-controlled trial has reported that ART has antiproliferative properties in colorectal cancer and is generally well tolerated in cancer patients.<sup>16</sup> Furthermore, combination of chemotherapy with ART leads to synergistic inhibition of tumor cell growth, which may improve clinical success rates in oncology.<sup>11</sup>

Traditional Chinese medicine herbs exert only few side effects and adverse events were less frequently reported than by conventional Western medicines due to its particular pharmacological properties and appropriate use by TCM clinical physicians.<sup>17-19</sup> The quintessence of TCM is the combination and interaction of different herbs in one formula, in which possible side effect exerted by one herb are neutralized by another herb in the herbal mixture, while the efficacy of each herb is synergistically enhanced. In fact, many herbal components have certain toxicities, causing damages on nervous, liver, renal, respiratory, and reproductive systems.<sup>20</sup> Without the interactions in formula, the use of single herbal components, such as ART, may bear some risks in clinical application and side effects may occur in cases of overdose. Recently, concerns about the safety of ART have been raised due to the potential toxicity observed during its treatment.<sup>21-23</sup> Therefore, in-depth knowledge on the pharmacological efficacy-safety profile of ART is urgently needed for its clinical application. Here, we hypothesized that ART's dosage may be a key factor that accounts for its efficacy-safety relationship, that is, ART may induce toxicity at high doses, but exerts safe efficacy at low doses. To verify this hypothesis, we applied a larval Zebrafish model to study the efficacy-toxicity relationship of ART.

Zebrafish (*Danio rerio*) is a small vertebrate belonging to the cyprinid teleost family. The adult Zebrafish reaches only 3 cm in length. During the embryonic and larval stages, it is only 2 to 3 mm long, which adapts to the assays on standard plates (96 or 384 wells/plate) with conventional nutrients.<sup>24</sup> Larval zebrafishes are used as an ideal model for testing the acute toxicity of compounds with several advantages compared to other mammal models.<sup>25</sup> In this study, we conducted in vivo experiments on larval Zebrafish to test the acute toxicity and efficacy of ART and performed RNA-sequencing analyses to unravel the underlying signaling pathways contributing to ART's activities.

## Materials and Methods

### Chemicals and Reagents

Artesunate (Batch number: B20992) with a purity of  $\geq 98\%$  was purchased as a powder from Shanghai Yuanye Biotechnology Co, Ltd (Shanghai, China). Verapamil hydrochloride (Batch number: K1629079) with a purity of  $\geq 98\%$  as a powder

was purchased from Shanghai Aladdin Reagent Co, Ltd (Shanghai, China). Dimethyl sulfoxide (DMSO) was obtained from Sigma-Aldrich (Taufkirchen, Germany). Trizol reagent was purchased from Takara Biotechnology Co, Ltd (Dalian, China). Artesunate and verapamil hydrochloride were dissolved with DMSO and ultrapure water for experimental use, respectively.

### Zebrafish Handling

Wide-type AB strain of Zebrafish was purchased from China Zebrafish Resource Center (CZRC), Institute of Hydrobiology, Chinese Academy of Sciences (Wuhan, China) and bred by Hunter Biotechnology, Inc. (Hangzhou, China). All zebrafishes were accredited by the Association for Assessment and Accreditation of Laboratory Animal Care (AAA LAC) International (SYXK2012-0171). After natural pair-mating and reproduction by adult zebrafishes, larval zebrafishes at the 2 days postfertilization stage (dpf) were generated and housed in a light-controlled aquaculture facility with a standard 14:10 hours day/night photoperiod and fed with live brine shrimp twice a day and dry flake once a day. The water temperature was maintained at 28°C (0.2% instant ocean salt, pH 6.9-7.2, conductivity 480-510  $\mu\text{S}/\text{cm}$ , and hardness 53.7~71.6 mg/L  $\text{CaCO}_3$ ).

### Determination of Maximum Nonlethal Concentration and Lethal Concentration 10% of ART

Totally 270 larval zebrafishes (2 dpf) were grouped (30 fishes per group) and distributed into 6-well plates in 3 mL fresh fish water for each well. Eight concentrations of ART (0, 5, 10, 20, 30, 40, 60, 80 ng/fish) were used to intravenous (IV) inject zebrafishes in each group. The injection volume was 2 nL/fish. Dead zebrafishes were daily recorded and removed. The dose-mortality response curve was generated by using Origin 8.0 (OriginLab, Northampton, Massachusetts). Maximum nonlethal concentration (MNLC) and Lethal concentration 10% ( $\text{LC}_{10}$ ) were determined by logistic regression calculation.

### Acute Toxicity Assay

To evaluate the acute toxicity of ART, 180 larval zebrafishes (2 dpf) were grouped ( $n = 30$ ) and IV injected with 1/9 MNLC, 1/3 MNLC, MNLC, and  $\text{LC}_{10}$  of ART as well as ultrapure water (normal control [NC] group) and DMSO (solvent control group) for 3 days, respectively. The injection volume was 2 nL/fish. After treatment, the heart, brain, mandible, eyes, liver, intestine, spine, muscle, color, blood circulation, and all abnormal symptoms of each Zebrafish were observed under the microscope. The occurrence of edema, hemorrhage, and thrombosis were also observed. All abnormal phenotypes were statistically recorded by double-blind evaluation.

**Table 1.** Primer Sequences Used for Real Time PCR Analysis.

Gene	Forward Primer	Reverse Primer
<i>18S</i>	5'-AGAGGGACAAGTGGCGTTCAG-3'	5'-TCAAGCCCCAGTCCCAATCAC-3'
<i>Fzd7a</i>	5'-TGCTCTCGTGC GGACTGTTAC-3'	5'-CGTTTGTTCACGCACAGT-3'
<i>Cdk5rap1</i>	5'-AGCAAACGATTTGGAACAGGC-3'	5'-GGCCCAGCTAGTACATCCAC-3'
<i>Ptges</i>	5'-TGGAGCGGTCTACTCCATGA-3'	5'-GCTGTGAAGAACTCGACCCA-3'
<i>Ndufa8</i>	5'-TCTAACATGGGTGAGCTGCG-3'	5'-GTTCCAGAAGAACAAGCGGC-3'

### Efficacy Assay of ART

To evaluate the cardioprotective effect of ART, acute heart failure model of zebrafish was established by in administration of verapamil hydrochloride. Totally 210 larval zebrafishes (2 dpf) were grouped (n = 30) and IV injected with 0, 1.25, 2.5, and 5 ng/fish of ART, respectively, for 3 days. The injection volume was 2 nL/fish. The heart area was observed under the dissecting microscopy (SZX7; Olympus, Tokyo, Japan), and the cardiac output, venous stasis, and blood flow rate were calculated and obtained with Heart Blood Flow Analysis System (Zebrolab3.3 PB2084C; ViewPoint, Ltd, Lyon, France). The bodies of zebrafishes were collected and 2 replicates were applied for RNA-sequencing analysis.

### RNA-Sequencing Analysis

Total RNA was isolated from zebrafishes by using Trizol reagent according to the instructions of the manufacturer and treated with RNase-free DNase I to remove the residual DNA. The quality and integrity of the RNA sample were confirmed using an Agilent 2100 Bioanalyzer (Agilent, Waldbronn, Germany). The concentration of total RNA was quantified using a NanoDrop 2000 spectrophotometer (Thermo Scientific, Massachusetts). For complementary DNA (cDNA) library preparation, 3 µg total RNA were captured by Dynabeads Oligo (dT) (Life Technologies, New York) and sheared to fragments of ~200 bp. Reverse transcription was performed by Superscript III cDNA Synthesis Kit. The cDNA was end-repaired, A-tailed and ligated to Illumina sequencing adapters and amplified by polymerase chain reaction (PCR). Library preparation was performed by TruSeq RNA LT V2 Sample Prep Kit (Illumina, San Diego, California). The sequencing library was qualified by Qubit 2.0 (Life technologies) and Agilent 2100 Bioanalyzer. The DNA sequencing was performed on the Illumina XTen Sequencing System (Illumina). Real-time image analysis and base calling were performed by HiSeq Control Software (HCS 1.5).

The raw data (raw reads) obtained from the Illumina HiSeq platform were processed by removing the adapters, sequences with uncertain bases, low-quality sequences, and sequences of less than 50 bp to generate clean data (clean reads). The clean reads from the Fastq files were mapped to the Zebrafish reference genome using the Spliced Transcripts Alignment to Reference (STAR) software. Differential expression analysis of the different groups was performed with biological replicates using the DESeq software. Value of *P* .05 was set as the

threshold for significant differential expression. To find the pathways which mediate ART's effect, analysis of Kyoto Encyclopedia of Genes and Genomes (KEGG) was performed. For the KEGG analysis, nonsupervised orthologous groups (eggNOG) database was used to cluster the genes into functionally related groups, followed by eMapper functional annotation. Then R language based clusterprofile package was used for KEGG enrichment analysis, and hypergeometric distribution test was conducted to determine the significance (*P* < .05) of enriched KEGG pathway.

### Real Time PCR (RT-PCR) Assay

Real Time PCR assay was performed to verify the expression of candidate genes by using an ABI QuantStudio 7 Flex Real-Time PCR System (Applied Biosystems, California). The total RNA of zebrafishes was extracted using Trizol reagent and synthesized to cDNA via reverse transcription. Real Time PCR reaction system had a 20.0 µL volume: 10.0 µL SYBR Premix Ex Taq II (Tli RnaseH Plus), 0.8 µL PCR Forward Primer, 0.8 µL PCR Reverse Primer, 2.0 µL template cDNA, 0.4 µL ROX Reference Dye, and 6.0 µL ddH<sub>2</sub>O. The reaction condition was set to 95°C for 30 seconds initial denaturation, 40 cycles of 95°C for 5 seconds denaturation, 60°C for 35 seconds annealing, and 72°C for 40 seconds extension. At the end of each reaction, a melting curve analysis was performed. Data were normalized to the expression of 18 S and presented by using 2<sup>-ΔΔCT</sup> method (Table 1).

## Results

### Acute Toxicity of ART

ART-induced dose-mortality curve was shown in Figure 1 (upper). No death of zebrafishes was observed within ART doses from 5 to 30 ng/fish, and no survival was seen with ART at dose of 80 ng/fish. Accordingly, MNLC and lethal dose 10% (LD<sub>10</sub>) were estimated as 32.4 and 41.8 ng/fish. During the double-blind observation, the lowest observed adverse effect level (LOAEL) of ART was estimated as 2.5 ng/fish. For acute toxicity assay, 1/9 of MNLC (3.6 ng/fish), 1/3 of MNLC (10.8 ng/fish), MNLC, and LD<sub>10</sub> were adopted.

As shown in Figure 1 (middle and lower), morphological abnormalities of zebrafishes were observed with ART treatments. In both NC and solvent control groups, abnormal phenotypes were not found in the zebrafishes. If treated with increasing ART doses, the incidences of abnormal

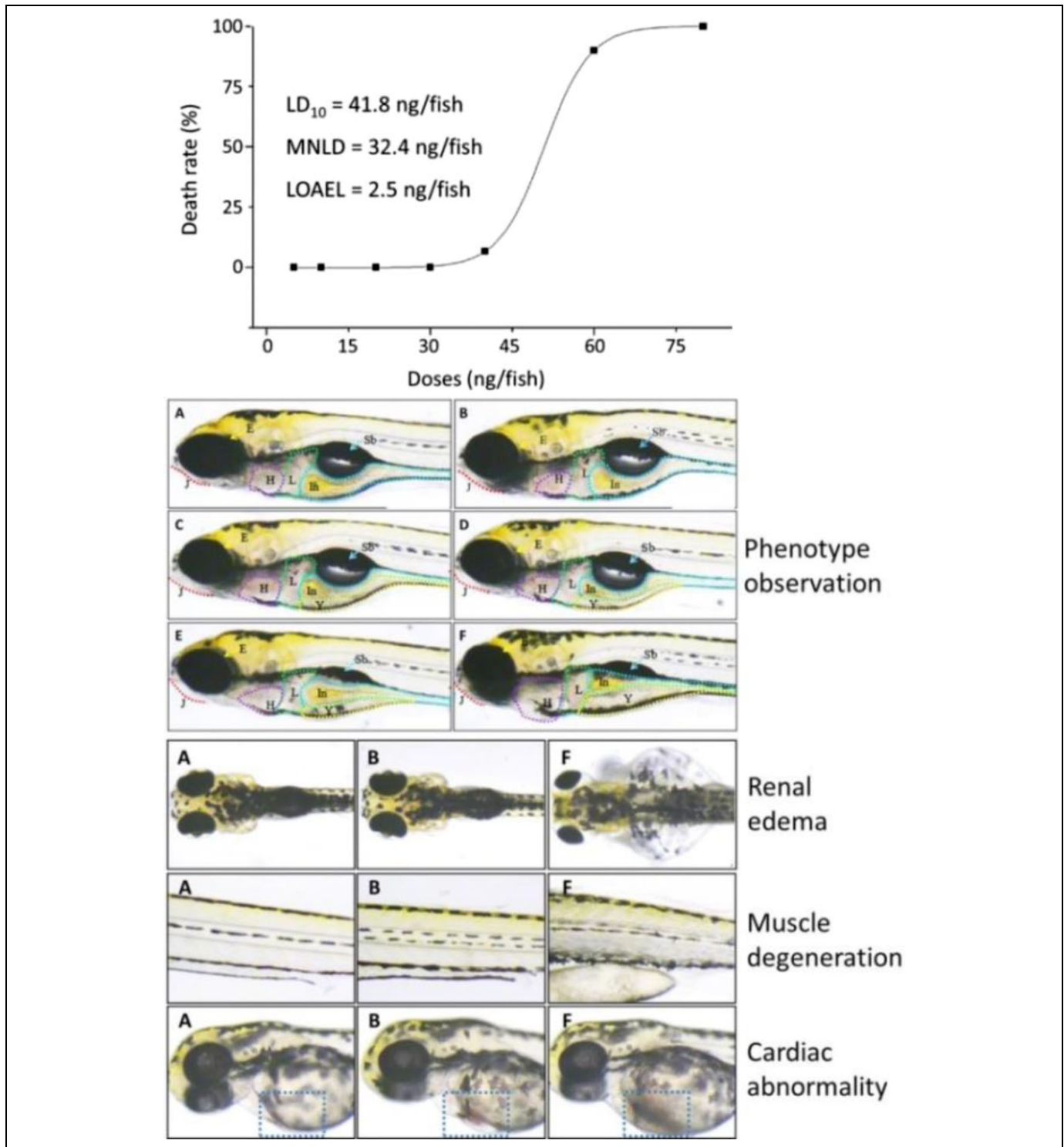


**Figure 1.** Acute toxicity observation of ART in zebrafishes. Upper: dose-mortality response curve with MNL and LD<sub>10</sub>; Middle: microscopic observation (J: mandible; E: eye; H: heart; L: liver; Y: yolk sac; In: intestine; Sb: swim bladder) on A: (normal control group); B: (solvent control group); C: (1/9 MNL ART treated group); D: (1/3 MNL ART treated group); E: (MNL ART treated group); and F: (LD<sub>10</sub> ART treated group); Lower: observation of renal edema, muscle degeneration (muscle texture abnormality), and cardiac abnormality. LD<sub>10</sub> indicates lethal dose 10%, MNL, maximum nonlethal concentration.

manifestations, such as pericardium edema, slowed circulation defect (venous stasis), and yolk sac absorption delay, were found mainly in the cardiovascular system of zebrafishes,

indicating dose-dependent acute toxicity of ART, especially cardiotoxicity. The hearts in these zebrafishes suffered from dilation and edema and were filled with turbid fluid, which

**Table 2.** Artesunate-Induced Abnormal Manifestations Their Occurrence Rate in Zebrafishes.<sup>a</sup>

Observable Abnormalities (Abnormal Fish/Total Fish)	NC	DMSO	ART (ng/fish)			
			3.6	10.8	32.4	41.8
Pericardium edema	—	—	2/30	2/30	4/30	7/30
Slowed heart rate	—	—	—	—	—	5/30
Circulation defect	—	—	3/30	7/30	10/30	29/30
Brain malformation	—	—	—	—	—	3/30
Mandible malformation	—	—	—	—	—	3/30
Eye shrink	—	—	—	—	—	3/30
Yolk sac absorption delay	—	—	18/30	22/30	25/30	27/30
Renal edema	—	—	—	—	1/30	3/30
Muscle degeneration	—	—	—	—	—	3/30
Body length decrease	—	—	—	—	—	3/30
Swim bladder loss	—	—	—	—	3/30	26/30

<sup>a</sup>“—” indicates 0/30.

seemed to be bigger than those of normal zebrafishes. Particularly, almost all fishes (incidence of >96%) suffered from circulation defects upon ART treatment at a dose of LD<sub>10</sub>. Artesunate at doses from MNLC to LD<sub>10</sub> caused severe renal edema and swim bladder loss, indicating acute nephrotoxicity and developmental toxicity. Besides, ART at LD<sub>10</sub> exerted toxicity in almost all organs in zebrafishes, including brain, mandible, eyes, muscle, and body length (Table 2).

### Cardioprotective Effect of ART

To determine the effective and safe dose range and verify the cardiotoxicity of ART, another acute toxicity assay was conducted with ART treatment at doses of 1.25, 2.5, and 5.0 ng/fish. As shown in Figure 2A, typical manifestation of cardiotoxicity, such as venous congestion and stasis, was observed in zebrafishes treated with 2.5 and 5.0 ng/fish ART. Thus, 1.25 ng/fish (1/2 LOAEL) was safe for the cardiovascular system and selected for the efficacy assay. As shown in Figure 2B and lower, heart dilatation, venous stasis, cardiac output decrease, and blood flow dynamics reduction were observed in zebrafishes treated with verapamil hydrochloride, of which treatment induced heart failure in 100% zebrafishes. No observable toxicity or death was found in zebrafishes after treatment of verapamil hydrochloride. After 1.25 ng/fish ART treatment, those verapamil-induced heart failure associated symptoms in zebrafishes were significantly restored toward normal levels (Figure 2B and lower panel), indicating a profound cardioprotective effect of ART at 1.25 ng/fish.

### RNA-Sequencing-Based Transcriptional Profile of ART

Nearly 56 to 76 million RNA-sequencing reads for zebrafishes in the NC, model, and ART groups were obtained. For expression measurements, more than 92% of total reads mapped to reference database genes. Statistical analysis revealed 630 (NC vs model) and 368 (model vs ART) differentially expressed genes ( $P < .05$ ) out of 31 476 reference genes. The top 50 significantly expressed genes, which are selected based on the

variance of gene expression level among the 3 groups, are shown in Figure 3. Of these, gene of frizzled class receptor 7a (*fzd7a*, gene id: gene41822) and gene of coronin 1Cb (*coro1cb*, gene id: gene13501) were significantly upregulated in the model group (adjusted  $P < .01$  vs NC) and downregulated in the ART group (adjusted  $P < .01$  vs model). Through KEGG-based pathway analysis, *fzd7a*-mediated Wnt signaling pathway was found to be mostly related to the heart failure modeling and ART treatment (Figure 4).

As shown in Table 3, besides *fzd7a*, there are many other genes participating in both the heart failure modeling and cardioprotective action of ART, including *Cdk5rap1*, *Creld2*, *Klotho*, *Ndufa8*, *Ptges*, *Slc22a17*, and *Stat6*. Of these genes, *Cdk5rap1*, *Klotho*, *Ptges*, and *Slc22a17* were significantly downregulated and *Creld2*, *Ndufa8*, and *Stat6* significantly upregulated by the heart failure modeling, while those abnormal changes were significantly reversed by ART. All the selected genes are related to the cardiac function of Zebrafish.

### Relative Messenger RNA Expression of Candidate Genes in Zebrafishes

Real time PCR was performed to assess the relative messenger RNA expression of selected candidate genes in zebrafishes. As shown in Figure 5, when compared with NC, *fzd7a* and *ndufa8* were significantly upregulated and *cdk5rap1* and *ptges* were significantly downregulated in the model group (each  $P < .01$ ). The expressions of these genes were significantly reversed toward the NC levels in the ART group (each  $P < .01$  vs model), verifying the RNA-seq results that those genes participated not only in the heart failure modeling but also the cardioprotective action of ART.

### Discussion

During the Vietnam War, numerous Vietnamese soldiers were dying from malaria and the Vietnamese government asked China for help. Then, the Chinese government launched a research project to search for antimalaria drugs from TCM.

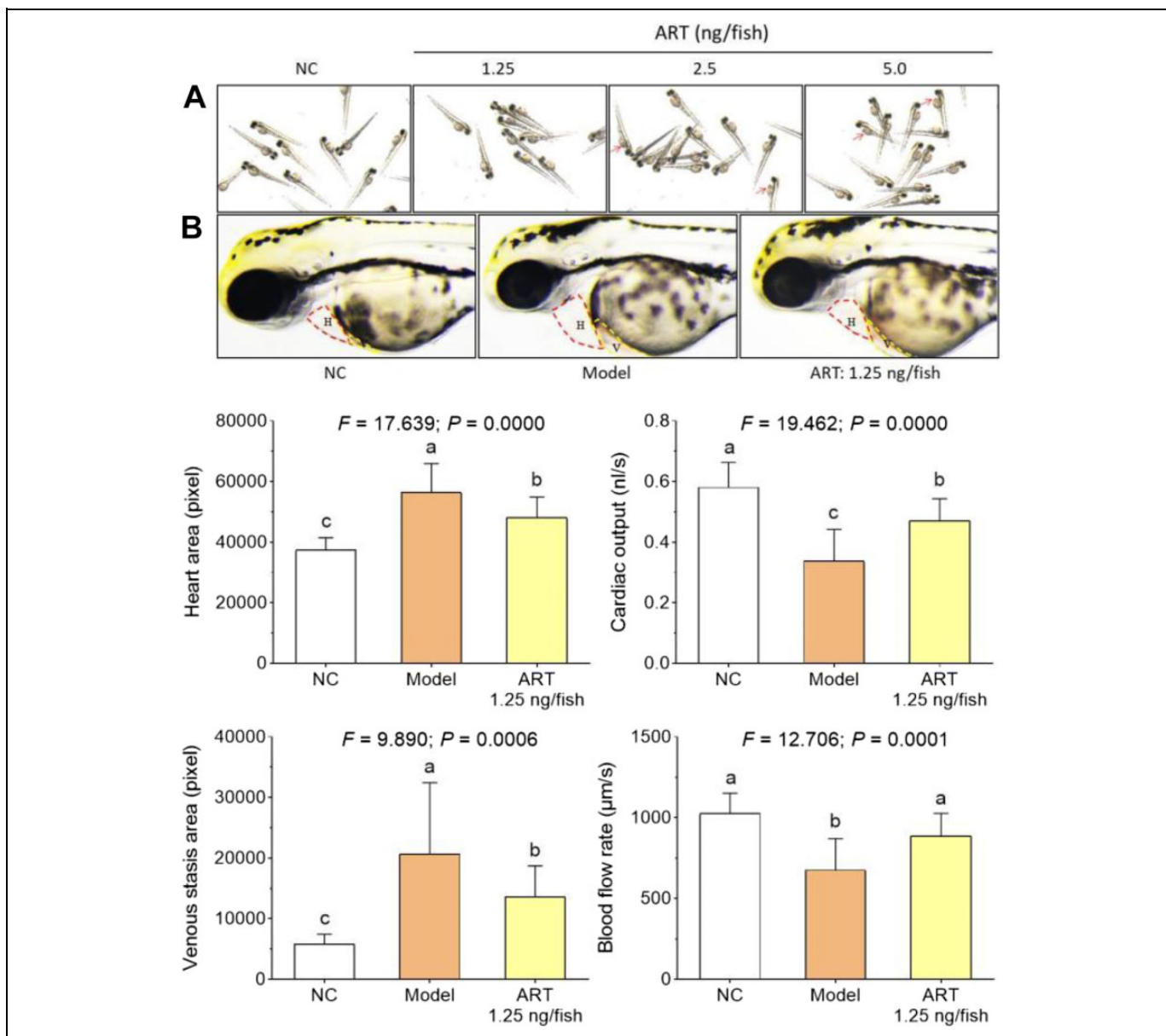


**Figure 2.** Cardiotoxicity and cardioprotective effect of ART in zebrafishes. (A) observation of circulation defect (venous congestion and stasis); (B) observation of heart failure phenotype. Lower: calculation of heart area, cardiac output, venous stasis, and blood flow rate. NC: normal control group; Model: acute heart failure group. Data (mean  $\pm$  SD) with different lowercase letters are significantly different with each other at LSD multiple comparisons. LSD indicates Fisher's least significant difference; SD, standard deviation.

As a result, artemisinin was screened out as a strong antimalaria compound from *A. annua* in 1972.<sup>44</sup> Subsequently, artemisinin was found to possess antitumor activity in a multispecific manner.<sup>10</sup> For instance, a metastasized stage-4 breast cancer patient revealed tumor regression in computer tomography upon artemisinin treatment, and another terminal hepatocellular carcinoma patient with abdominal ascites was still alive 2.5 years after taking artemisinin.<sup>45</sup> However, artemisinin is not soluble in water; thereby it is not appropriate for intramuscular or IV injection, which seriously restrains its effect in clinic.<sup>8</sup> Besides, considerable toxicities were found

with artemisinin in the majority of animal experiments and in clinical applications, indicating dose limitations of this compound for treatment of diseases.<sup>21,46</sup> To overcome this shortcoming, ART has been synthesized as the only clinical applicable water-soluble derivative of artemisinin, which exerts better effect with lesser toxicity than other derivatives.<sup>47</sup> The World Health Organization (WHO) has strongly recommended parenteral (intramuscular or IV) ART as first-line treatment for severe malaria.<sup>48</sup> Two large randomized clinical trials showed a 35% reduction in death rates in adults in Asia and a 22.5% reduction in children in Africa, if ART was

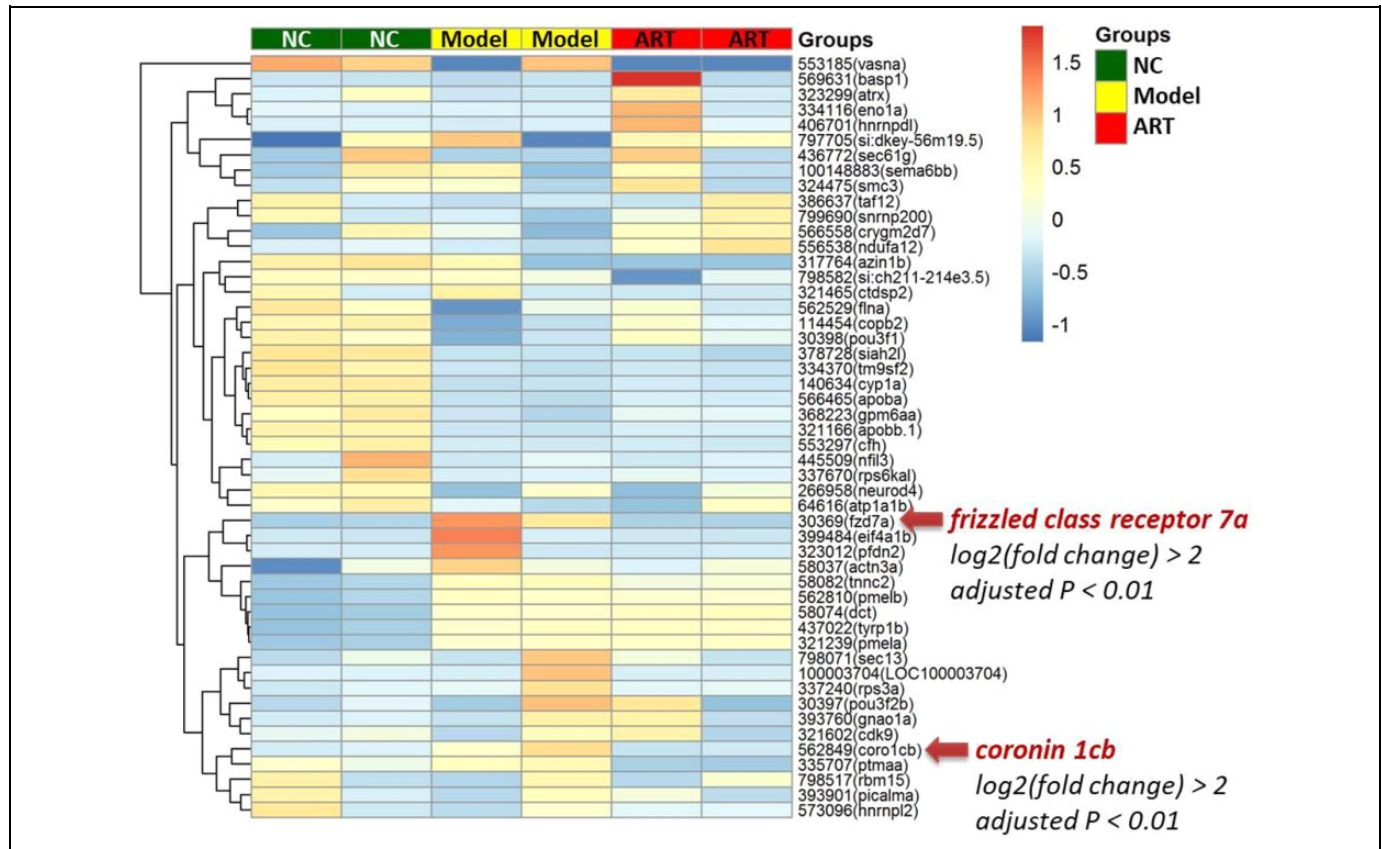


**Figure 3.** Heat map overview of the top 50 significantly expressed genes in zebrafishes.

compared with Quinine.<sup>49,50</sup> Besides, a clinical trial in advanced non-small cell lung cancer reported a higher disease control rate and a longer survival time of the ART-treated patients, and another clinical trial reported apoptosis-inducing and recurrence-preventive effect of ART in colorectal carcinoma patients.<sup>51,16</sup> However, clinical data reported that adverse events, including delayed hemolysis, arterial ischemia, abnormal cardiac manifestations, neurological syndromes, renal dysfunction, hypertension, and hyperkalemia, were related to ART treatment.<sup>5</sup> Delayed hemolysis and arterial ischemia were the most frequent reported adverse events in ART-treated patients (about 20%), which may cause cardiovascular complications.<sup>52,53</sup> This raises concerns about potential toxicity of ART on the cardiovascular system. The WHO guideline indicated that individual parenteral ART doses between 1.75 and 4 mg/kg had no toxicity.<sup>48</sup> Therefore, we hypothesized that different doses of ART may exert different or even contrary effects.

To verify this hypothesis, we applied the larval Zebrafish model to conduct acute toxicity and efficacy assays. Larval Zebrafish represents a well-established animal model, which suitably serves for toxicity assessment. It offers many advantages compared to traditional *in vivo* and *in vitro* models, such as: (1) optically large and transparent body for real-time observation of organ response; (2) high sensitivity to toxic insults; (3) similar cellular and molecular processes as human beings; (4) high-throughput application and less experimental time due

to high fecundity and rapid development; and (5) low overall costs.<sup>54-56</sup> Optical transparency and sensitivity to toxic agents render the larval Zebrafish a very suitable organism for early prediction of drug toxicity and efficacy in comparison to rodents and other larger animals. The overall predictive success rate of zebrafishes for drug-induced toxicity attained 100%, being ranked as excellent (>85%) by the European Center for the Validation of Alternative Methods (ECVAM) criteria.<sup>57,58</sup> Particularly, Zebrafish has been served as an excellent model for assessing drug-induced cardiotoxicity and cardioprotection, although Zebrafish and mammalian hearts differ in structure.<sup>59-61</sup> Seven known human cardiotoxic drugs (aspirin, clomipramine hydrochloride, cyclophosphamide, nimodipine, quinidine, terfenadine, and verapamil hydrochloride) and 2 noncardiotoxic drugs (gentamicin sulphate and tetracycline hydrochloride) have been assessed by using Zebrafish, in which all the cardiotoxic drugs induced cardiotoxicity and no sign of cardiotoxicity was found with the noncardiotoxic drugs.<sup>62</sup> The overall prediction success rate for cardiotoxic drugs and noncardiotoxic drugs in Zebrafish were 100% as compared with human results, suggesting Zebrafish as an excellent model for rapid *in vivo* cardiotoxicity screening.<sup>62</sup> Moreover, our previous report has firstly revealed the cardiotoxicity of a known noncardiotoxic agent, sodium aescinate, by using larval Zebrafish, suggesting Zebrafish as an assessment model not only for known

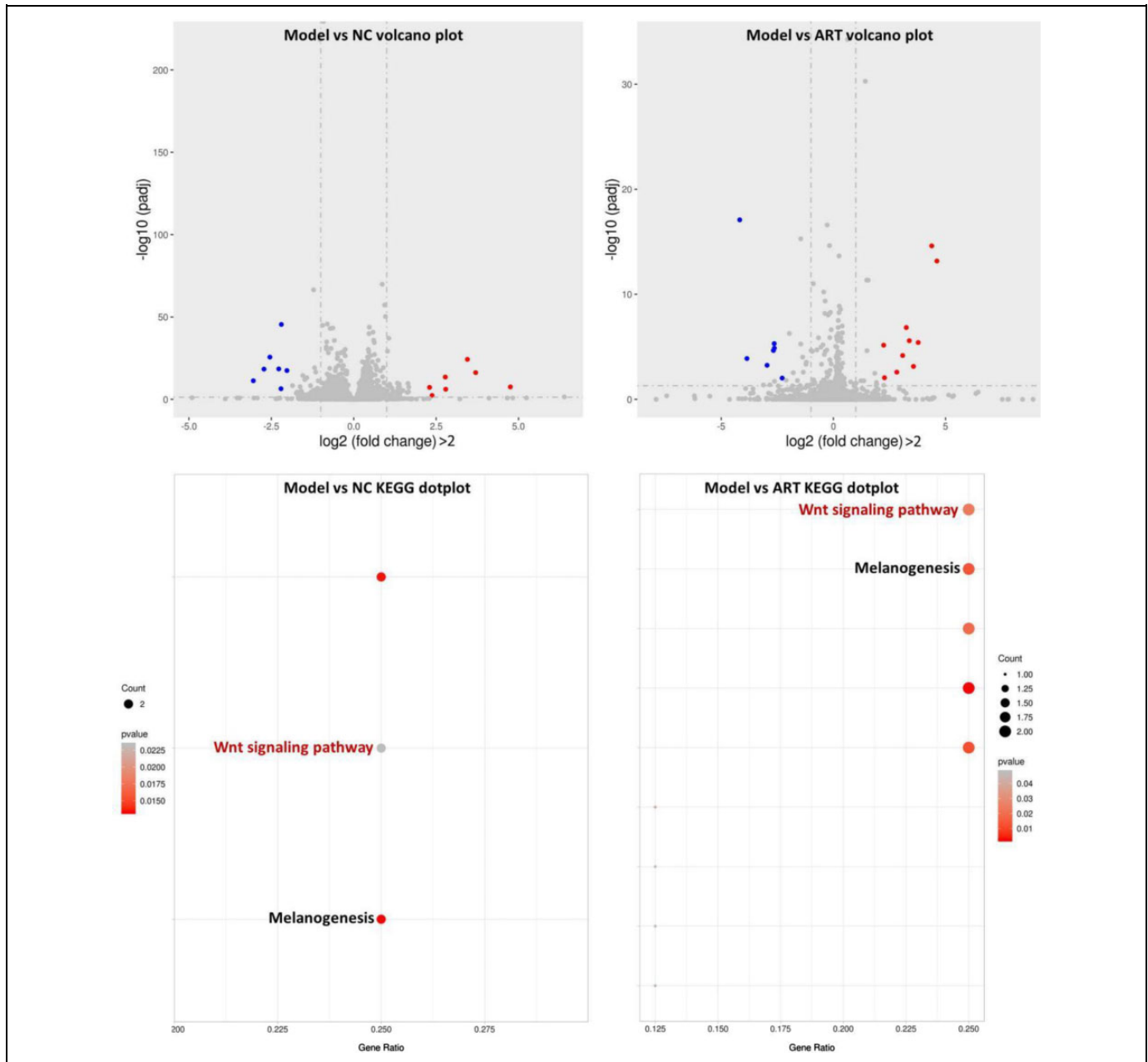


**Figure 4.** Volcano plot and KEGG pathways for the comparison between the different treatment groups as assayed by RNA-sequencing analysis. KEGG Kyoto Encyclopedia of Genes and Genomes.

**Table 3.** Significantly Expressed Genes Which Are Related to Cardiotoxicity or Cardioprotection.

Genes	Model vs NC			Model vs ART			Functions
	$\log_2(\text{Fold Change})$	lfc SE	P Value	$\log_2(\text{Fold Change})$	lfc SE	P Value	
<i>Cdk5rap1</i>	-4.44	1.94	.022	-4.13	1.94	.033	Cell cycle progression and cell growth <sup>26,27</sup>
<i>Klotho</i>	-2.52	0.88	.004	-1.82	0.89	.040	Cardioprotection <sup>28-34</sup>
<i>Ptges</i>	-6.48	2.91	.030	-6.98	2.91	.016	Cardioprotection <sup>35-37</sup>
<i>Slc22a17</i>	-2.70	0.92	.003	-2.41	0.92	.009	Cardiotoxicity <sup>38,39</sup>
<i>Creld2</i>	4.66	1.78	.009	4.42	1.77	.012	Cardiac defects <sup>40</sup>
<i>Ndufa8</i>	4.83	1.83	.008	5.36	1.84	.004	Pericardial edema <sup>41,42</sup>
<i>Stat6</i>	3.83	1.18	.001	2.31	0.96	.015	Cardiac injury and myocardial infarction <sup>43</sup>

Abbreviation: SE for  $\log_2(\text{fold change})$ .



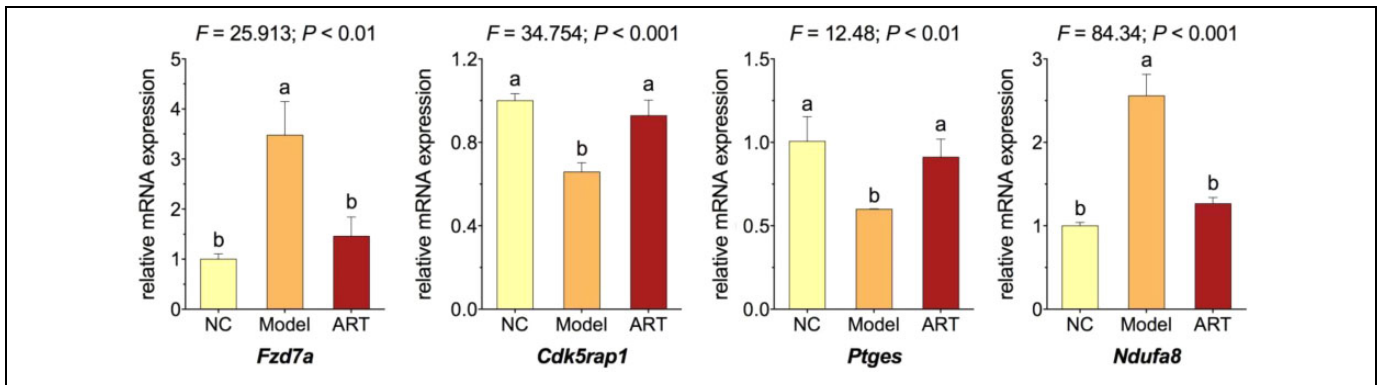


**Figure 5.** Relative messenger RNA expression of candidate genes in zebrafishes. Data (mean  $\pm$  SD) with different lowercase letters are significantly different with each other at multiple comparisons. SD indicates standard deviation.

cardiotoxicity but also for undiscovered cardiotoxicity.<sup>25</sup> Interestingly, Zebrafish have a unique ability to repair heart muscle, which raises particular concern regarding the interference of self-regeneration to its assessment of cardiotoxicity or cardioprotection. Indeed, such interference can be ignored because the regeneration will not occur within 7 to 14 days after myocardial injury and only 3 days are chosen as the end point for observation of cardiotoxicity and cardioprotection.<sup>63</sup> Therefore, Zebrafish can be regarded as a suitable model for rapid prediction of ART's cardiotoxicity and cardioprotection.

Our results from the acute toxicity assay showed that a single-dose IV injection of ART from 1/9 MNLC to above doses exerted obvious toxicity in the cardiovascular system, resulting in pericardial edema and circulation defects. Besides this obvious cardiotoxicity, ART at nonlethal doses ( $\leq$  MNLC) also exerted acute nephrotoxicity and developmental toxicity. Since the average body weight of the larval zebrafishes was 25 mg, the toxic dose range (1/9 MNLC to LD<sub>10</sub>) can be estimated as 0.144 to 0.932 mg/kg in Zebrafish, which could be extrapolated to 0.0144 to 0.0932 mg/kg in human beings.<sup>64</sup> The recommended daily doses of ART in clinical practice are 1.2 to 2.4 mg/kg human body weight, which is overwhelmingly higher than the above toxic doses extrapolated by the larval Zebrafish assay. The assay discovered such toxicity within 3 days after single injection of ART, indicating that single IV injection of ART potentially induces acute toxicity in its clinical doses for at least 3 days. However, it is generally known that ART is well tolerated and appears to be a safe option even during pregnancy. This controversy to our result can be explained by the following reason: Zebrafish is a very sensitive model suitable for the discovery of potential toxicity or side effects of therapeutics, and ART's toxicity might have been underestimated due to its invisibility in the clinic. On the other hand, ART at 1/2 LOAEL exerted cardioprotective effects on zebrafishes with heart failure, which significantly restored cardiac malformation, venous stasis, cardiac output decrease, and blood flow dynamics reduction. No adverse events were observed with this treatment, indicating that ART at doses below LOAEL was effective and safe. For the first time, the

above results revealed the efficacy-toxicity relationship of ART and verified our hypothesis that ART's dosage decides, whether it is toxic or effective. Such a biphasic dose-response relationship has been described as "hormesis," which refers to a phenomenon that is characterized by a "low-dose activation and high-dose inhibition".<sup>65,66</sup> In the context of ART, there was also a hormetic duality in response by zebrafishes in reply to an impetus that spurred favorable effects at a low dose and harmful effects at higher doses.

The RNA-sequencing result showed that 7 genes (*Cdk5rap1*, *Crel2*, *Klotho*, *Ndufa8*, *Ptges*, *Slc22a17*, and *Stat6*) contributed to both the development of heart failure and the cardioprotective effect of ART in Zebrafish. *Cdk5rap1* encodes cyclin-dependent kinase 5 regulatory subunit associated protein 1 which postsynthetically converts the RNA modification N6-isopentenyladenosine (i<sup>6</sup>A) into 2-methylthio-N6-isopentenyladenosine (ms<sup>2</sup>i<sup>6</sup>A). The expression of *Cdk5rap1* gene is related to the regulation and progression of the M phase of the cell cycle.<sup>26</sup> It has been reported that down-regulation of *Cdk5rap1* gene suppressed cell growth, arrested the cells at G2/M phase, and induced cell apoptosis through reactive oxygen species/c-Jun N-terminal kinase signaling pathway.<sup>27</sup> *Klotho* has been identified as an aging suppressor, encoding a  $\beta$ -glucuronidase-related antisenescence protein involved in cardiovascular diseases.<sup>28</sup> It acts as a cardioprotective factor in maintenance of cardiovascular homeostasis by suppressing vascular endothelial dysfunction, delaying vascular calcification, correcting sinoatrial node function and cardiac rhythm, and protecting heart from cardiac hypertrophy, senescence, and damage.<sup>29-31</sup> As demonstrated previously in humans, higher plasma klotho levels are independently related to a lower likelihood of cardiovascular disease events,<sup>32</sup> and in contrast, reduced systemic klotho levels are related to cardiovascular damage.<sup>33</sup> The expression of *Klotho* gene is decreased during aging or in response to other pathogens, which appears to play a critical role in the pathogenesis of cardiovascular diseases.<sup>28</sup> Inactivation of *Klotho* gene causes serious disorders, such as vascular endothelial dysfunction, atherosclerosis, diffuse vascular calcification, and cardiac hypertrophy.<sup>34</sup> *Ptges* encodes microsomal prostaglandin (PG) E<sub>2</sub> synthase-1

(mPGES-1) to catalyze PGE<sub>2</sub> biosynthesis and is expressed by cardiac myocytes and cardiac fibroblasts.<sup>35</sup> Inactivation of *Ptges* gene induces lack of mPGES-1, leading to eccentric cardiomyocyte hypertrophy, impaired left ventricle contractile function, adverse left ventricle remodeling, and increased severity of acute myocardial infarction.<sup>36,37</sup> *Slc22a17* encodes solute carrier family 22 member, a specific lipocalin2 receptor involved in many physiological and pathological processes such as cell differentiation, apoptosis, and inflammation.<sup>38</sup> Inactivation of *Slc22a17* gene has been found significantly associated with cardiotoxicity in clinic.<sup>39</sup> *Creld2* encodes the second member of the CRELD (cysteine rich with EGF-like domains) family proteins, which may be associated with cardiac atrioventricular septal defects.<sup>40</sup> *Ndufa8* encodes NADH dehydrogenase in complex I of the mitochondrial membrane respiratory chain. Activation of *Ndufa8* gene is associated with pericardial edema and mitochondrial damage.<sup>41,42</sup> *Stat6* encodes signal transducer and activator of transcriptional 6 (STAT6) protein, which is activated with cardiovascular diseases such as cardiac injury, ischemia and reperfusion events, and myocardial infarction.<sup>43</sup> In sum, downregulation of *Cdk5rap1*, *Klotho*, *Ptges*, and *Slc22a17* and upregulation of *Creld2*, *Ndufa8*, and *Stat6* by heart failure modeling in this study were probably associated with cardiotoxicity or cardiovascular disease events in Zebrafish, and ART exerted cardioprotective effects by reversing the abnormal expressions of those genes (Table 3). Since ART at high dose exerted a reversed effect (cardiotoxicity) in Zebrafish, in future, it is necessary to test the expression of those or some other candidate genes in Zebrafish treated with either high or low doses of ART and compare the expression patterns of the candidate genes in different dose conditions.

Furthermore, the gene expression of a transmembrane modulator of Wnt signaling pathway, Frizzled class receptor 7a, was significantly upregulated in heart failure zebrafishes and significantly downregulated by ART at 1/2 LOAEL, indicating that Wnt signaling pathway might mediate the cardioprotective effect of ART. As a classic signaling pathway, Wnt signaling plays an essential role in cardiac disease and serves as an important target for cardiac medication.<sup>67</sup> Artesunate has been reported to exert antimalaria and anticancer effects by inhibiting Wnt signaling pathway,<sup>68,69</sup> indicating Wnt signaling as a target for the treatments of ART. Interestingly, the Wnt signaling pathway also mediates the cardiotoxic effects of other therapeutic agents, such as doxorubicin (DOX). DOX is an effective chemotherapeutic agent in treating human neoplasms such as leukemia, lymphomas, and solid tumors.<sup>70</sup> Acute cardiotoxicity has been recognized as a severe complication with DOX chemotherapy, often resulting in congestive heart failure and irreversible degenerative cardiomyopathy.<sup>71</sup> The cardiotoxicity of DOX was mediated by Wnt signaling in cardiomyocytes.<sup>72</sup> Secreted frizzled-related proteins (sFRP) are ligands that bind to Fz receptors such as Frizzled class receptor 7a.<sup>73</sup> It can relieve DOX-induced cardiotoxicity by modulation of Wnt signaling.<sup>74,75</sup> Therefore, the fact that ART exerts a sFRP-like effect on the cardiovascular disease by targeting Frizzled class

receptor 7a in Wnt signaling indicates a therapeutic potential of ART for relieving DOX-induced cardiotoxicity in cancer treatment. It has been reported that some other herbal medicines have successfully alleviated cardiotoxicity in DOX-treated mice with cancer, providing a potential alternative treatment for cancer patients under DOX treatment.<sup>76</sup> It remains to be investigated in the future, whether the potential cardioprotective effects of ART can be exploited to reduce DOX-mediated cardiotoxicity in combination treatment protocols.

### Authors' Note

Chuanrui Zheng and Letian Shan contributed equally to this manuscript; they conceived of and designed this study, and wrote the article. Peijian Tong improved the design. Thomas Efferth improved the design, draft, and language editing of this manuscript. All listed authors approved the manuscript for publication and agreed to be accountable for all aspects of this work.



### Declaration of Conflicting Interests

The author(s) declared no potential conflicts of interest with respect to the research, authorship, and/or publication of this article.

### Funding

The author(s) disclosed receipt of the following financial support for the research, authorship, and/or publication of this article: This study was funded by the National Natural Science Foundation of China (Grant No: 81774331).

### ORCID iD

Chuanrui Zheng  <https://orcid.org/0000-0001-8935-3563>  
Letian Shan  <https://orcid.org/0000-0003-4926-0527>

### Supplemental Material

Supplemental material for this article is available online.

### References

1. China Pharmacopeia Committee. *Pharmacopeia of the People's Republic of China (the First Division)*. Beijing: China Chemical Industry Press; 2015, pp 198.
2. Neill US. From branch to bedside: youyou Tu is awarded the 2011 Lasker~DeBakey clinical medical research award for discovering artemisinin as a treatment for malaria. *J Clin Invest*. 2011; 121(10):3768-3773.
3. Efferth T, Zacchino S, Georgiev MI, Liu L, Wagner H, Panossian A. Nobel prize for artemisinin brings phytotherapy into the spotlight. *Phytomedicine*. 2015;22(13):A1-3.
4. Tu Y. Artemisinin—a gift from traditional Chinese medicine to the world (Nobel Lecture). *Angew Chem Int Ed Engl*. 2016; 55(35):10210-10226.
5. Roussel C, Caumes E, Thellier M, Ndour PA, Buffet PA, Jauréguiberry S. Artesunate to treat severe malaria in travellers: review of efficacy and safety and practical implications. *J Travel Med*. 2017;24(2).
6. Jiang W, Cen Y, Song Y, et al. Artesunate attenuated progression of atherosclerosis lesion formation alone or combined with rosuvastatin through inhibition of pro-inflammatory cytokines and

- pro-inflammatory chemokines. *Phytomedicine*. 2016;23(11):1259-1266.
7. Saeed MEM, Krishna S, Greten HJ, Kreamsner PG, Efferth T. Antischistosomal activity of artemisinin derivatives in vivo and in patients. *Pharmacol Res*. 2016;110:216-226.
  8. Zuo S, Li Q, Liu X, Feng H, Chen Y. The potential therapeutic effects of artesunate on stroke and other central nervous system diseases. *Biomed Res Int*. 2016;2016:1489050.
  9. Daddy NB, Kalisya LM, Bagire PG, Watt RL, Towler MJ, Weathers PJ. *Artemisia annua* dried leaf tablets treated malaria resistant to ACT and i.v. artesunate: case reports. *Phytomedicine*. 2017;32:37-40.
  10. Efferth T. From ancient herb to modern drug: *Artemisia annua* and artemisinin for cancer therapy. *Semin Cancer Biol*. 2017;46:65-83.
  11. Efferth T. Cancer combination therapy of the sesquiterpenoid artesunate and the selective EGFR-tyrosine kinase inhibitor erlotinib. *Phytomedicine*. 2017;37:58-61.
  12. Abba ML, Patil N, Leupold JH, Saeed MEM, Efferth T, Allgayer H. Prevention of carcinogenesis and metastasis by artemisinin-type drugs. *Cancer Lett*. 2018;429:11-18.
  13. Efferth T. Beyond malaria: the inhibition of viruses by artemisinin-type compounds. *Biotechnol Adv*. 2018;36(6):1730-1737.
  14. Naß J, Efferth T. The activity of *Artemisia spp.* and their constituents against trypanosomiasis. *Phytomedicine*. 2018;47:184-191.
  15. He RR, Zhou HJ. Progress in research on the anti-tumor effect of artesunate. *Chin J Integr Med*. 2008;14(4):312-316.
  16. Krishna S, Ganapathi S, Ster IC, et al. A randomised, double blind, placebo-controlled pilot study of oral artesunate therapy for colorectal cancer. *EBioMedicine*. 2014;2(1):82-90.
  17. Normile D. The new face of traditional Chinese medicine. *Science*. 2003;299(5604):188-190.
  18. Drasar P, Moravcova J. Recent advances in analysis of Chinese medical plants and traditional medicines. *J Chromatogr B Analyt Technol Biomed Life Sci*. 2004;812(1-2):3-21.
  19. Li WL, Zheng HC, Bukuru J, De Kimpe N. Natural medicines used in the traditional Chinese medical system for therapy of diabetes mellitus. *J Ethnopharmacol*. 2004;92(1):1-21.
  20. Wu T, Yu GY, Xiao J, et al. Fostering efficacy and toxicity evaluation of traditional Chinese medicine and natural products: Chick embryo as a high throughput model bridging in vitro and in vivo studies. *Pharmacol Res*. 2018;133:21-34.
  21. Efferth T, Kaina B. Toxicity of the antimalarial artemisinin and its derivatives. *Crit Rev Toxicol*. 2010;40(5):405-421.
  22. Uhl M, Schwab S, Efferth T. Fatal liver and bone marrow toxicity by combination treatment of dichloroacetate and artesunate in a glioblastoma multiforme patient: case report and review of the literature. *Front Oncol*. 2016;6:204.
  23. Efferth T, Schöttler U, Krishna S, Schmiedek P, Wenz F, Giordano FA. Hepatotoxicity by combination treatment of temozolomide, artesunate and Chinese herbs in a glioblastoma multiforme patient: case report review of the literature. *Arch Toxicol*. 2017;91(4):1833-1846.
  24. Peterson RT, Macrae CA. Systematic approaches to toxicology in the zebrafish. *Annu Rev Pharmacol Toxicol*. 2012;52:433-453.
  25. Liang J, Jin W, Li H, et al. In vivo cardiotoxicity induced by sodium aescinate in zebrafish larvae. *Molecules*. 2016;21(3):190.
  26. Padua MB, Hansen PJ. Changes in expression of cell-cycle-related genes in PC-3 prostate cancer cells caused by ovine uterine serpin. *J Cell Biochem*. 2009;107(6):1182-1188.
  27. Wang H, Wei L, Li C, Zhou J, Li Z. CDK5RAP1 deficiency induces cell cycle arrest and apoptosis in human breast cancer cell line by the ROS/JNK signaling pathway. *Oncol Rep*. 2015;33(3):1089-1096.
  28. Ding HY, Ma HX. Significant roles of anti-aging protein klotho and fibroblast growth factor23 in cardiovascular disease. *J Geriatr Cardiol*. 2015;12(4):439-447.
  29. Yao Y, Wang Y, Zhang Y, Liu C. Klotho ameliorates oxidized low density lipoprotein (ox-LDL)-induced oxidative stress via regulating LOX-1 and PI3K/Akt/eNOS pathways. *Lipids Health Dis*. 2017;16(1):77.
  30. Guo Y, Zhuang X, Huang Z, et al. Klotho protects the heart from hyperglycemia-induced injury by inactivating ROS and NF-kappaB-mediated inflammation both in vitro and in vivo. *Biochim Biophys Acta Mol Basis Dis*. 2018;1864(1):238-251.
  31. Baghaiee B, Karimi P, Siahkoughian M, Pescatello LS. Moderate aerobic exercise training decreases middle-aged induced pathologic cardiac hypertrophy by improving Klotho expression, MAPK signaling pathway, and oxidative stress status in Wistar rats. *Iran J Basic Med Sci*. 2018;21(9):911-919.
  32. Semba RD, Cappola AR, Sun K, et al. Plasma klotho and cardiovascular disease in adults. *J Am Geriatr Soc*. 2011;59(9):1596-1601.
  33. Navarro-García JA, Fernández-Velasco M, Delgado C, et al. PTH, vitamin D, and the FGF-23-klotho axis and heart: going beyond the confines of nephrology. *Eur J Clin Invest*. 2018;48(4).
  34. Santiago JJ, McNaughton LJ, Koleini N, et al. High molecular weight fibroblast growth factor-2 in the human heart is a potential target for prevention of cardiac remodeling. *PLoS One*. 2014;9(5):e97281.
  35. Giannico G, Mendez M, LaPointe MC. Regulation of the membrane-localized prostaglandin E synthases mPGES-1 and mPGES-2 in cardiac myocytes and fibroblasts. *Am J Physiol Heart Circ Physiol*. 2005;288(1):H165-H174.
  36. Degousee N, Simpson J, Fazel S, et al. Lack of microsomal prostaglandin E(2) synthase-1 in bone marrow-derived myeloid cells impairs left ventricular function and increases mortality after acute myocardial infarction. *Circulation*. 2012;125(23):2904-2913.
  37. Degousee N, Fazel S, Angoulvant D, et al. Microsomal prostaglandin E2 synthase-1 deletion leads to adverse left ventricular remodeling after myocardial infarction. *Circulation*. 2008;117(13):1701-1710.
  38. Cabedo Martínez AI, Weinhäupl K, Lee WK, et al. Biochemical and structural characterization of the interaction between the siderocalin NGAL/LCN2 (neutrophil gelatinase-associated lipocalin/lipocalin 2) and the N-terminal domain of its endocytic receptor SLC22A17. *J Biol Chem*. 2016;291(6):2917-2930.
  39. Visscher H, Rassekh SR, Sandor GS, et al. Genetic variants in SLC22A17 and SLC22A7 are associated with

- anthracycline-induced cardiotoxicity in children. *Pharmacogenomics*. 2015;16(10):1065-1076.
40. Maslen CL, Babcock D, Redig JK, Kapeli K, Akkari YM, Olson SB. CRELD2: gene mapping, alternate splicing, and comparative genomic identification of the promoter region. *Gene*. 2006;382:111-120.
  41. AshaRani PV, Low Kah Mun G, Hande MP, Valiyaveetil S. Cytotoxicity and genotoxicity of silver nanoparticles in human cells. *ACS Nano*. 2009;3(2):279-290.
  42. Zou W, Zhou Q, Zhang X, Mu L, Hu X. Characterization of the effects of trace concentrations of graphene oxide on zebrafish larvae through proteomic and standard methods. *Ecotoxicol Environ Saf*. 2018;159:221-231.
  43. Wincewicz A, Sulkowski S. Stat proteins as intracellular regulators of resistance to myocardial injury in the context of cardiac remodeling and targeting for therapy. *Adv Clin Exp Med*. 2017;26(4):703-708.
  44. Tu Y. The development of new antimalarial drugs: qinghaosu and dihydro-qinghaosu. *Chin Med J (Engl)*. 1999;112(11):976-977.
  45. Rowen RJ, editor. *Breakthroughs for Preventing and Surviving Cancer*. Atlanta, GA: Second Opinion Publishing Inc; 2002.
  46. Ndagije HB, Nambasa V, Manirakiza L, et al. The burden of adverse drug reactions due to artemisinin-based antimalarial treatment in selected Ugandan health facilities: an active follow-up study. *Drug Saf*. 2018;41(8):753-765.
  47. Clark RL, Brannen KC, Sanders JE, Hoberman AM. Artesunate and arteminic acid: association of embryotoxicity, reticulocytopenia, and delayed stimulation of hematopoiesis in pregnant rats. *Birth Defects Res B Dev Reprod Toxicol*. 2011;92(1):52-68.
  48. World Health Organization. *Guidelines for the Treatment of Malaria*. 3rd ed. Geneva, Switzerland: World Health Organization; 2015.
  49. Dondorp A, Nosten F, Stepniewska K, Day N, White N; South East Asian Quinine Artesunate Malaria Trial (SEAQUAMAT) Group. Artesunate versus quinine for treatment of severe falciparum malaria: a randomised trial. *Lancet*. 2005;366(9487):717-725.
  50. Dondorp AM, Fanello CI, Hendriksen IC, et al. Artesunate versus quinine in the treatment of severe falciparum malaria in African children (AQUAMAT): an open-label, randomised trial. *Lancet*. 2010;376(9753):1647-1657.
  51. Zhang ZY, Yu SQ, Miao LY, et al. Artesunate combined with vinorelbine plus cisplatin in treatment of advanced non-small cell lung cancer: a randomized controlled trial [in Chinese]. *ZhongXi Yi Jie He Xue Bao*. 2008;6(2):134-138.
  52. Gómez-Junyent J, Ruiz-Panales P, Calvo-Cano A, Gascón J, Muñoz J. Delayed haemolysis after artesunate therapy in a cohort of patients with severe imported malaria due to *Plasmodium falciparum* [English, Spanish]. *Enferm Infecc Microbiol Clin*. 2017;35(8):516-519.
  53. Jauréguiberry S, Thellier M, Ndour PA, et al; French Artesunate Working Group. Delayed onset hemolytic anemia in patients with travel-associated severe malaria treated with artesunate, France, 2011-2013. *Emerg Infect Dis*. 2015;21(5):804-812.
  54. Hill AJ, Teraoka H, Heideman W, Peterson RE. Zebrafish as a model vertebrate for investigating chemical toxicity. *Toxicol Sci*. 2005;86(1):6-19.
  55. McGrath P, Li CQ. Zebrafish: a predictive model for assessing drug-induced toxicity. *Drug Discov Today*. 2008;13(9-10):394-401.
  56. Vliegenthart AD, Tucker CS, Del Pozo J, Dear JW. Zebrafish as model organisms for studying drug-induced liver injury. *Br J Clin Pharmacol*. 2014;78(6):1217-1227.
  57. Burns CG, Milan DJ, Grande EJ, Rottbauer W, MacRae CA, Fishman MC. High-throughput assay for small molecules that modulate zebrafish embryonic heart rate. *Nat Chem Biol*. 2005;1(5):263-264.
  58. Ducharme NA, Reif DM, Gustafsson JA, Bondesson M. Comparison of toxicity values across zebrafish early life stages and mammalian studies: implications for chemical testing. *Reprod Toxicol*. 2015;55:3-10.
  59. Lee SH, Kim HR, Han RX, Oqani RK, Jin DI. Cardiovascular risk assessment of atypical antipsychotic drugs in a zebrafish model. *J Appl Toxicol*. 2013;33(6):466-470.
  60. Shi X, Verma S, Yun J, et al. Effect of empagliflozin on cardiac biomarkers in a zebrafish model of heart failure: clues to the EMPA-REG OUTCOME trial? *Mol Cell Biochem*. 2017;433(1-2):97-102.
  61. Zakaria ZZ, Benslimane FM, Nasrallah GK, et al. Using zebrafish for investigating the molecular mechanisms of drug-induced cardiotoxicity. *Biomed Res Int*. 2018;2018:1642684.
  62. Zhu JJ, Xu YQ, He JH, et al. Human cardiotoxic drugs delivered by soaking and microinjection induce cardiovascular toxicity in zebrafish. *J Appl Toxicol*. 2014;34(2):139-148.
  63. Chablais F, Veit J, Rainer G, Jazwińska A. The zebrafish heart regenerates after cryoinjury-induced myocardial infarction. *BMC Dev Biol*. 2011;11:21.
  64. Zhang C, Willett C, Fremgen T. Zebrafish: an animal model for toxicological studies. *Curr Protoc Toxicol*. 2003;Chapter 1: Unit1.7.
  65. Calabrese V, Cornelius C, Trovato A, et al. The hormetic role of dietary antioxidants in free radical-related diseases. *Curr Pharm Des*. 2010;16(7):877-883.
  66. Bhakta-Guha D, Efferth T. Hormesis: decoding two sides of the same coin. *Pharmaceuticals (Basel)*. 2015;8(4):865-883.
  67. Stylianidis V, Hermans KCM, Blankesteyn WM. Wnt signaling in cardiac remodeling and heart failure. *Handb Exp Pharmacol*. 2017;243:371-393.
  68. Li LN, Zhang HD, Yuan SJ, Tian ZY, Wang L, Sun ZX. Artesunate attenuates the growth of human colorectal carcinoma and inhibits hyperactive Wnt/beta-catenin pathway. *Int J Cancer*. 2007;121(6):1360-1365.
  69. Zheng L, Pan J. The anti-malarial drug artesunate blocks Wnt/ $\beta$ -catenin pathway and inhibits growth, migration and invasion of uveal melanoma cells. *Curr Cancer Drug Targets*. 2018;18(10):988-998.
  70. Sant M, Allemani C, Santaquilani M, Knijn A, Marchesi F, Capocaccia R; EURO CARE Working Group. EURO CARE-4. Survival of cancer patients diagnosed in 1995-1999. Results and commentary. *Eur J Cancer*. 2009;45(6):931-991.

71. Hayek ER, Speakman E, Rehmus E. Acute doxorubicin cardiac toxicity. *N Engl J Med.* 2005;352(23):2456-2457.
72. Xie Z, Xia W, Hou M. Long intergenic non-coding RNA-p21 mediates cardiac senescence via the Wnt/ $\beta$ -catenin signaling pathway in doxorubicin-induced cardiotoxicity. *Mol Med Rep.* 2018;17(2):2695-2704.
73. Malinauskas T, Jones EY. Extracellular modulators of Wnt signalling. *Curr Opin Struct Biol.* 2014;29:77-84.
74. Hu Y, Guo Z, Lu J, et al. sFRP1 has a biphasic effect on doxorubicin-induced cardiotoxicity in a cellular location-dependent manner in NRCMs and rats. *Arch Toxicol.* 2019; 93(2):533-546.
75. Merino H, Singla DK. Secreted Frizzled-related protein-2 inhibits doxorubicin-induced apoptosis mediated through the Akt-mTOR pathway in soleus muscle. *Oxid Med Cell Longev.* 2018;2018: 6043064.
76. Lien CY, Chuang TY, Hsu CH, et al. Oral treatment with the herbal formula B307 alleviates cardiac toxicity in doxorubicin-treated mice via suppressing oxidative stress, inflammation, and apoptosis. *Oncotargets Ther.* 2015;8:1193-1210.